# Functional Analysis of the Copper-Dependent Quercetin 2,3-Dioxygenase. 1. Ligand-Induced Coordination Changes Probed by X-ray Crystallography: Inhibition, Ordering Effect, and Mechanistic Insights†

Roberto A. Steiner,‡ Ingeborg M. Kooter,§ and Bauke W. Dijkstra*,‡

*Laboratory of Biophysical Chemistry, Department of Chemistry, University of Groningen, Nijenborgh 4, 9747 AG Groningen, The Netherlands, and Unilever Research Vlaardingen, Olivier van Noortlaan 120, 3133 AT Vlaardingen, The Netherlands*

*Received November 26, 2001; Revised Manuscript Received May 7, 2002*

ABSTRACT: The crystal structures of the copper-dependent *Aspergillus japonicus* quercetin 2,3-dioxygenase (2,3QD) complexed with the inhibitors diethyldithiocarbamate (DDC) and kojic acid (KOJ) are reported at 1.70 and 2.15 Å resolution, respectively. Both inhibitors asymmetrically chelate the metal center and assume a common orientation in the active site cleft. Their molecular plane blocks access to the inner portion of the cavity which is lined by the side chains of residues Met51, Thr53, Phe75, Phe114, and Met123 and which is believed to bind the flavonol B-ring of the natural substrate. The binding of the inhibitors brings order into the mixed coordination observed in the native enzyme. DDC and KOJ induce a single conformation of the Glu73 side chain, although in different ways. In the presence of DDC, Glu73 is detached from the copper ion with its carboxylate moiety pointing away from the active site cavity. In contrast, when KOJ is bound, Glu73 ligates the Cu ion through its $O^{\epsilon 1}$ atom with a monodentate geometry. Compared to the native coordinating conformation, this conformation is approximately 90° rotated about the $\chi_3$ angle. This latter Glu73 conformation is compatible with the presence of a bound substrate.

Dioxygenases are enzymes that catalyze the incorporation of both atoms of molecular oxygen into organic substrates. They take part in the metabolism of biomolecules as different as amino acids, lipids, nucleic acids, and even carbohydrates (*1*). Their biological importance relates in particular, however, to their ability to catalyze the degradation of aromatic compounds (*1*−*3*).

Dioxygenases are often mononuclear non-heme iron-containing enzymes (*4*). In the thoroughly investigated extradiol- and intradiol-type catechol dioxygenases, structural and spectroscopic studies have elucidated how the iron center is exploited to accomplish catalysis (for reviews, see refs *2* and *5*). Extradiol-type dioxygenases utilize an $Fe^{2+}$ ion to ligate and to directly activate $O_2$, whereas the intradiol-type enzymes employ $Fe^{3+}$ to activate their substrate prior to dioxygen attack. Although their employed strategies are different, both enzyme types utilize the metal cofactor to circumvent the spin barrier that prohibits the direct reaction of ground-state triplet dioxygen with singlet-state organic substrates.

Dioxygenases containing other metal centers (Cu (*6*−*9*), Mn (*10*), Mg (*11*)) have also been reported. They have, however, not been studied as extensively as the iron-containing enzymes. Quercetin 2,3-dioxygenase (2,3QD)[1] is the only dioxygenase unambiguously known to contain copper (*7*, *9*). It cleaves the *O*-heterocycle of polyphenolic flavonols (Figure 1a) which represent a major class of flavonoids (*12*). These compounds are important dietary components and have attracted considerable attention in the past decade owing to their antioxidizing properties (*13*−*15*).

Recently, our group has elucidated the X-ray structure of 2,3QD from *Aspergillus japonicus* at 1.6 Å resolution (PDB code 1JUH (*16*)) providing the first structural view of a non-iron dioxygenase. The enzyme is a homodimer of ∼100 kDa. The dimerization is probably not of functional relevance because the copper centers are about 40 Å apart, and no residues from the other subunit are nearby. The monomer contains two domains, an N-terminal domain (residues 1−145) and a C-terminal domain (residues 206−350), which are joined by a long stretch of 60 amino acids (residues 146−205). The two domains share a common jelly roll motif. A large shallow hydrophobic cavity located in the N-terminal domain hosts the metallocenter. On the basis of a sequence analysis and its three-dimensional fold, the enzyme has been found to belong to the cupin superfamily (*16*).

The coordination environment of the copper ion in 2,3QD is complex (Figure 2a). The metal is chiefly bound in a distorted tetrahedral geometry by three histidine residues

† The research described here was supported by The Netherlands Foundation for Chemical Research (CW) with the financial aid from The Netherlands Foundation for Scientific Research (NWO). The EU supported the work at the synchrotron sites through the HCMP Access to Large Installations Program.

* Corresponding author. Phone: +31-50-3634381. Fax: +31-50-3634800. E-mail: bauke@chem.rug.nl.

‡ University of Groningen.

§ Unilever Research Vlaardingen.

[1] Abbreviations: 2,3QD, quercetin 2,3-dioxygenase; DDC, sodium diethyldithiocarbamate; EPR, electron paramagnetic resonance; E·S, enzyme·flavonol complex; EXAFS, extended X-ray absorption fine structure; KOJ, kojic acid (5-hydroxy-2-(hydroxymethyl)-4*H*-pyran-4-one); QUE, quercetin (5,7,3′,4′-tetrahydroxy flavonol); XAS, X-ray absorption spectroscopy.

10.1021/bi0159736 CCC: $22.00 
Published on Web 06/01/2002

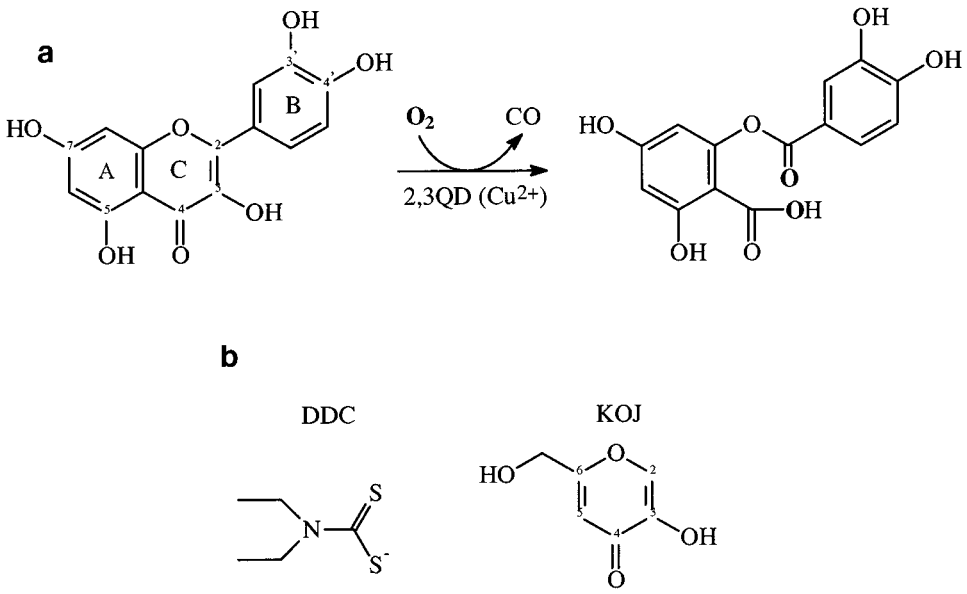


FIGURE 1: Scheme of 2,3QD-mediated dioxygenation of the flavonol substrate quercetin (3,5,7,3′,4′-pentahydroxy flavone). (a) Flavonol ring and atom nomenclature is given in the left-hand part. (b) Representation of the molecular structures of diethyldithiocarbamate (DDC) and kojic acid (KOJ).

(His66, His68, and His112) and a water molecule ($Wat_{td}$). However, a minor trigonal bipyramidal/square pyramidal coordination is also observed, in which the water molecule ($Wat_{tb}$) is positioned somewhat further away from the Cu ion ($Cu-Wat_{tb}$ = 2.4 Å, $Cu-Wat_{td}$ = 2.2 Å) and the side chain of Glu73 additionally coordinates the metal. The latter coordination is particularly interesting because carboxylate ligation has never before been observed in natural copper proteins (*18*−*20*).

To date, no structural data are available on 2,3QD substrate or inhibitor complexes. In this report, we present the crystal structures of 2,3QD inhibited with diethydithiocarbamate (2,3QD·DDC) along with that of its complex with kojic acid (2,3QD·KOJ). The molecular structures of DDC and KOJ are presented in Figure 1b. Our crystallographic study shows the molecular basis for a common inhibitory mode and indicates that the binding of these effectors induces order in the copper coordination. Additionally, valuable mechanistic insights, particularly on the role of Glu73, are inferred from this work.

## MATERIALS AND METHODS

*2,3QD Preparation and Purification.* 2,3QD was overexpressed and purified as previously described (*16*). Protein purity was ascertained by SDS−PAGE gel electrophoresis. The metal site was found to be fully occupied by atomic absorption spectrometry using a Perkin-Elmer model Plasma 1000.

*Crystallization and Soaking Experiments.* For crystallization purposes, the purified 2,3QD glycoenzyme (ca. 25% carbohydrate content, w/w) was treated with Endoglycosidase-H (Boehringer-Mannheim, Almere, The Netherlands) following the protocol indicated by the manufacturer. The released carbohydrates were removed by gel filtration chromatography on a Pharmacia Superdex G75 column. This procedure reduced the residual glycosylation to about 3−5% (w/w). An activity assay, carried out according to the procedure of Oka et al. (*21*), indicated that the deglycosylation had no adverse effect on the catalytic efficiency of 2,3QD.

Crystals of DDC inhibited 2,3QD were obtained by cocrystallizing the enzyme with the inhibitor at room temperature using the hanging-drop method. The protein solution (15 mg/mL in 50 mM MES buffer, pH 6.0) was mixed in a 1:1 ratio with a reservoir solution containing PEG8000 (21−23% w/v), 200 mM ammonium sulfate, 100 mM sodium citrate (pH 5.2), and 10 mM DDC. Crystals belonging to space group $P2_1$ grew in about 3 weeks. 2,3QD, complexed with KOJ, was obtained by soaking crystals of 2,3QD for 12 h in a reservoir solution identical to that described previously except for the substitution of the DDC by 50 mM KOJ. The crystals of the complexes are isomorphous to those of the native enzyme.

*Data Collection and Refinement of the Models.* Diffraction data were collected from a 2,3QD·DDC crystal using synchrotron radiation at beam line BW7B (EMBL, Hamburg, Germany) employing a MAR345 image plate detector (MAR Research, Hamburg, Germany). Intensities from a crystal of 2,3QD·KOJ were collected at beam line BM14 (EMBL, Grenoble, France) using the same type of detector. Both data collections were carried out at 100 K. A total of 25% (v/v) MPD was used as a cryo-protectant. Integration, scaling, and merging of the data was done with the HKL suite (*22*). Data collection and processing results together with the final refinement statistics are summarized in Table 1. The relatively high $R_{sym}$ value of 13% of the 2,3QD·KOJ data set is the result of the poor quality of the single crystal which still diffracted after the soaking procedure and from which a full data could be obtained. Restrained refinement of both models including TLS refinement (*23*, *24*) was performed with the program REFMAC5 (*25*, *26*). Initial phases were obtained from the model of native 2,3QD at 1.6 Å (PDB code 1JUH) from which all of the nonprotein atoms and residue Glu73 were removed. No restraints on the metal−ligand distances were used. An estimate of the occupancies of the ligands was obtained from their refinement using the

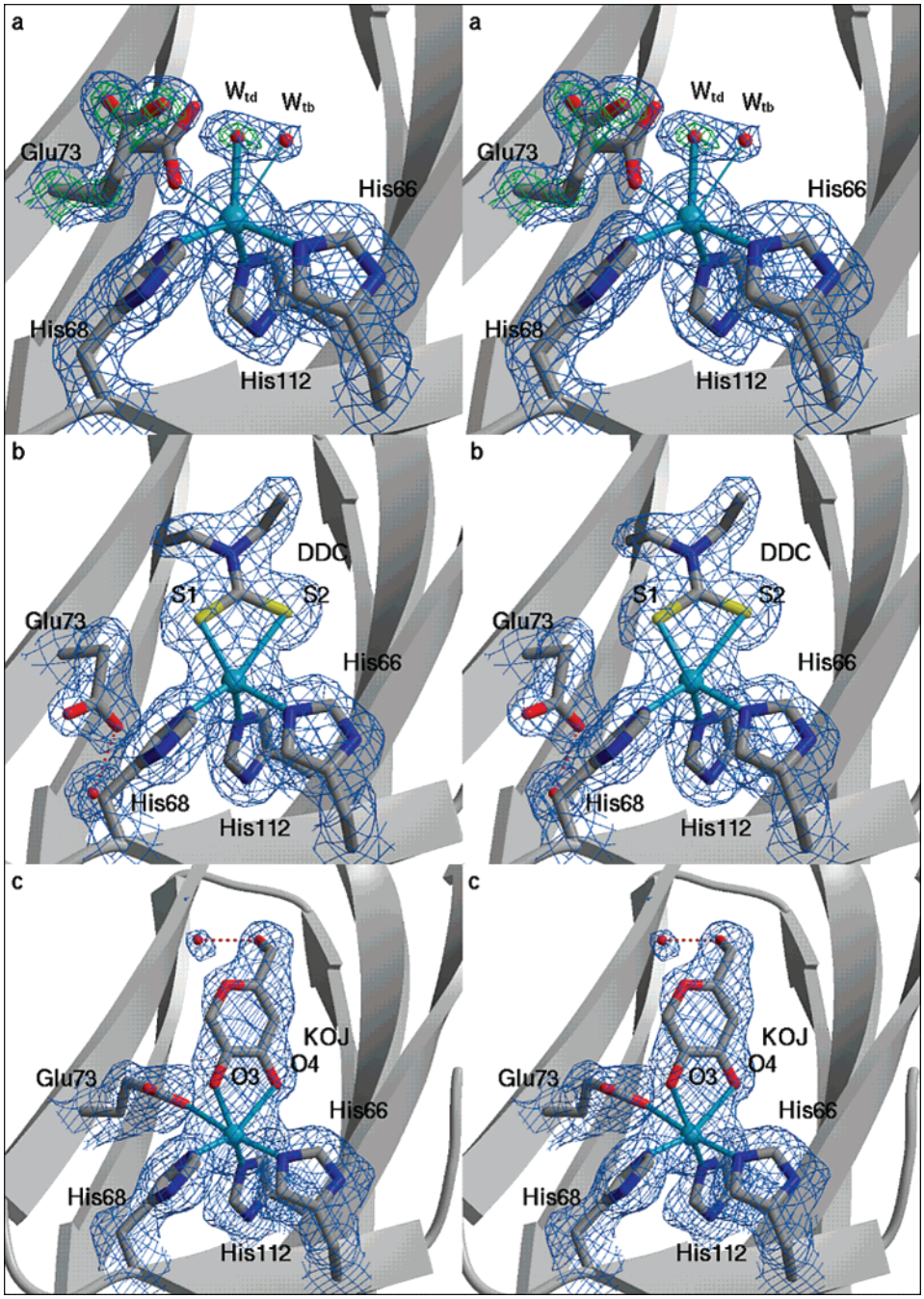


FIGURE 2: Stereoview of the active site of (a) native 2,3QD, (b) 2,3QD·DDC, and (c) 2,3QD·KOJ. $2F_o - F_c$ electron density is contoured at 1.0$\sigma$ (blue) and 2.5$\sigma$ (green, only for Glu73 and the solvent molecule in part a). Coordination details are given in Table 2. Histidine residues 66, 68, and 112 bind to the metal through their $N^{\epsilon 2}$ atoms. Glu73 binds through its $O^{\epsilon 1}$ atom. This figure was generated with the programs BOBSCRIPT (*38*) and RASTER3D (*39*).

program CNX (Accelrys Inc., Burlington, MA). The molecular model of DDC was obtained from the Cambridge Structural Database (*27*), whereas that of KOJ was generated and minimized using the routines incorporated in the program QUANTA (Accelrys Inc., Burlington, MA).

*Analysis of the Models.* Map inspections and rebuilding were carried out with the programs QUANTA and XTALVIEW (*28*). The stereochemical quality of the final structures was assessed with the program PROCHECK (*29*).

*Accession Numbers.* Atomic coordinates and structure factors have been deposited with the Protein Data Bank, RCSB Rutgers University, with the entry codes 1gqg and 1gqh, and r1gqgsf and r1gqhsf, respectively.

## RESULTS

*Crystal Structure of 2,3QD·DDC.* DDC is a known chelating agent of $Cu^{2+}$ ions and strongly inhibits 2,3QD at concentrations as low as $10^{-7}$ M (*9*, *30*). DDC binds in the active site region and ligates to the copper ion. Its two sulfur atoms loosely occupy the two alternate positions of the water molecule bound in the native structure (Figure 2a,b), and its plane extends toward the two antiparallel $\beta$-strands formed by residues 46−55 and 120−130, respectively. It interacts with Tyr35, Glu73, Phe75, Phe114, Met123, Ile127, and Phe132 mainly through van der Waals contacts of its alkyl side chains (Figure 3a).

Table 1: Data Collections and Refinement Statistics

| | | |
|---|---|---|
| **Data Collection** | | |
| data set | 2,3QD·DDC | 2,3QD·KOJ |
| source | BW7B (DESY) | BM14 (ESRF) |
| detector | MAR345 | MAR345 |
| $T$ (K) | 100 | 100 |
| wavelength (Å) | 0.845 | 1.033 |
| resolution range (Å) | 20.0−1.70 | 50.0−2.15 |
| space group | $P2_1$ | $P2_1$ |
| molecules in the a.u. | 4 | 4 |
| cell dimensions | | |
| $a$ (Å) | 108.94 | 108.64 |
| $b$ (Å) | 55.65 | 55.40 |
| $c$ (Å) | 123.86 | 124.43 |
| $\beta$ (deg) | 98.26 | 98.26 |
| no. observations | 637 059 | 150 878 |
| no. unique | 148 198 | 72 101 |
| completeness (%) | 91.1 (69.4) | 89.2 (86.5) |
| $R_{symm}$ (%)[a] | 6.2 (17.3) | 13.0 (37.6) |
| $\langle I\rangle/\langle\sigma(I)\rangle$ | 18.1 (4.5) | 7.03 (3.0) |
| $B$ value (Å$^2$)[b] | 23.5 | 23.1 |
| **Refinement** | | |
| $R_{factor}$ (%)[a] | 16.1 | 17.7 |
| $R_{free}$ (%)[a] | 18.4 | 22.8 |
| coordinate error (Å)[c] | 0.067 | 0.152 |
| $B$ values error (Å$^2$)[c] | 2.0 | 5.7 |
| rms bond lengths (Å)[d] | 0.009 | 0.010 |
| rms bond angles (deg)[d] | 1.3 | 1.4 |
| **Final Model** | | |
| no. non-H atoms | 12 136 | 11 751 |
| no. protein residues | 1334 | 1339 |
| no. copper ions | 4 | 4 |
| no. carbohydrate residues | 21 | 25 |
| no. ligand molecules | 4 | 4 |
| no. water molecules | 1444 | 1020 |
| average $B$ all atoms (Å$^2$) | 28.1 | 22.5 |
| average $B$ protein (Å$^2$) | 26.6 | 21.6 |
| average $B$ Cu (Å$^2$) | 28.4 | 22.5 |
| average $B$ carbohydrates (Å$^2$) | 39.0 | 35.1 |
| average $B$ ligand (Å$^2$) | 29.9 | 38.4 |
| average $B$ water molecules (Å$^2$) | 36.2 | 26.6 |
| **Ramachandran Plot** | | |
| no. most favored $\varphi,\psi$ (%) | 88.2 | 86.0 |
| no. favored $\varphi,\psi$ (%) | 10.8 | 13.0 |
| no. additionally favored $\varphi,\psi$ (%) | 1.0 | 0.9 |
| no. disallowed $\varphi,\psi$ (%) | 0.0 | 0.1 |

[a] For the definitions of standard crystallographic quantities, the reader is referenced to ref *35*. $R_{free}$ (*36*) was calculated using 5% of the data. [b] Estimated $B$ value from Wilson statistics. [c] Estimated errors are derived from maximum likelihood. [d] rms deviations from ideality (*37*).

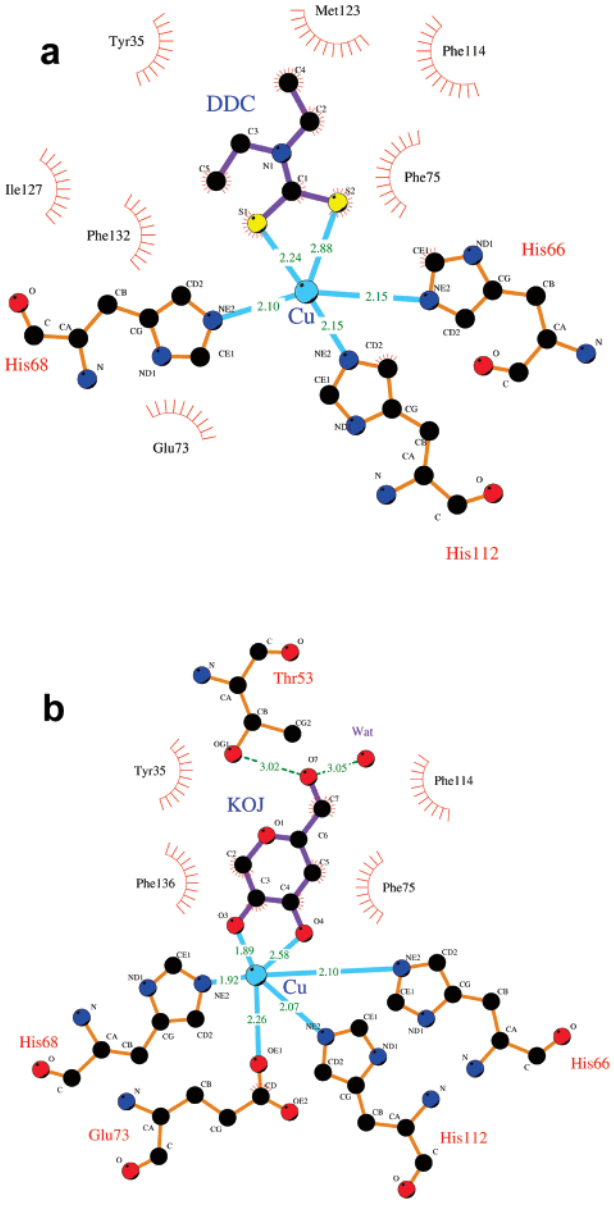


FIGURE 3: LIGPLOT (*40*) representation of (a) DDC-2,3DQ and (b) KOJ-2,3QD interactions.

The DDC coordination is pronouncedly asymmetrical. One sulfur atom (DDC$^{S1}$) is at an average distance of 2.2 Å from the copper, whereas the other sulfur (DDC$^{S2}$) is further away at 2.9 Å. The latter sulfur is positioned roughly trans to His68 forming an His68$^{N\epsilon2}$−Cu−DDC$^{S2}$ angle of 152°. In contrast, DDC$^{S1}$ is opposite to His66 with an His66$^{N\epsilon2}$−Cu−DDC$^{S1}$ angle of 143°. The coordination geometry at the copper is a distorted square pyramid. His112 is the apical ligand, whereas the two sulfur atoms of DDC, His66$^{N\epsilon2}$ and His68$^{N\epsilon2}$, form the base plane. The copper ion is displaced from this plane by about 0.5 Å in the direction of His112$^{N\epsilon2}$. As often observed in pentacoordinated sites, the square pyramidal geometry is distorted toward a trigonal bipyramidal arrangement in which the His66$^{N\epsilon2}$, His112$^{N\epsilon2}$, and DDC$^{S1}$ atoms form the equatorial plane and DDC$^{S2}$ and His68$^{N\epsilon2}$ are the apical ligands. To quantitate the extent of the distortion, the $\tau$ parameter (*31*) has been employed as a measure of the degree of trigonality. For a perfectly square pyramidal geometry, $\tau$ is zero, while it becomes one in the case of a perfect trigonal bipyramidal geometry. Calculation of the $\tau$ index for this site gives a value of 0.29 in accordance with the more square pyramidal character of the coordination geometry. In contrast, the pentacoordinated geometry of native 2,3QD has a $\tau$ of 0.63, indicating a more trigonal bipyramidal character.

The three-dimensional structure of 2,3QD·DDC is virtually identical to that of native 2,3QD. The average rms deviation for the superposition of 1288 C$^\alpha$ atoms of the four molecules present in the asymmetric unit is 0.19 Å only. However, despite their general similarity, a major difference is present at the active site. The flexible Glu73 residue which coordinates the copper in one of its alternate conformations in the native enzyme is no longer in the copper coordination sphere in 2,3QD·DDC (Figure 3b). DDC binding induces a new noncoordinating conformation different from that observed in the native enzyme. In this conformation, the Glu73 side chain has its C$^\gamma$−C$^\delta$ bond almost parallel to the main chain, with $\chi_1 = -58°$ (−110° in 2,3QD), $\chi_2 = 73°$ (−80°), and

Table 2: Coordination Geometries[a]

| atoms | data set geometry/ligands: 2,3QD tetrahedral/ His66, His68, His112, $W_{td}$ | 2,3QD trigonal bipyramidal/ His66, His68, Glu73, His112, $W_{tb}$ | 2,3QD·DDC square pyramidal/ His66, His68, His112, DDC | 2,3QD·KOJ octahedral/ His66, His68, Glu73, His112, KOJ |
|---|---|---|---|---|
| | | Distances (Å) | | |
| Cu−$His66^{N\epsilon 2}$ | 2.16 (0.02) | 2.16 (0.02) | 2.15 (0.06) | 2.10 (0.10) |
| Cu−$His68^{N\epsilon 2}$ | 2.09 (0.02) | 2.09 (0.02) | 2.10 (0.05) | 1.92 (0.09) |
| Cu−$Glu^{O\epsilon 1}$ | | 2.10 (0.08) | | 2.26 (0.18) |
| Cu−$His112^{N\epsilon 2}$ | 2.10 (0.04) | 2.10 (0.04) | 2.15 (0.02) | 2.07 (0.06) |
| Cu−$W^{tb}$ | | 2.41 (0.21) | | |
| Cu−$W^{t}$ | 2.21 (0.02) | | | |
| Cu−$DDC^{S1}$ | | | 2.24 (0.07) | |
| Cu−$DDC^{S2}$ | | | 2.88 (0.07) | |
| Cu−$KOJ^{O3}$ | | | | 1.89 (0.15) |
| Cu−$KOJ^{O4}$ | | | | 2.58 (0.30) |
| | | Angles (deg) | | |
| $His66^{N\epsilon 2}$−Cu−$His68^{N\epsilon 2}$ | 99 (1) | 99 (1) | 92 (3) | 99 (5) |
| $His66^{N\epsilon 2}$−Cu−$Glu73^{O\epsilon 1}$ | | 174 (4) | | 171 (4) |
| $His66^{N\epsilon 2}$−Cu−$His112^{N\epsilon 2}$ | 95 (1) | 95 (1) | 91 (2) | 96 (3) |
| $His66^{N\epsilon 2}$−Cu−$W^{tb}$ | | 94 (5) | | |
| $His66^{N\epsilon 2}$−Cu−$W^{t}$ | 109 (1) | | | |
| $His66^{N\epsilon 2}$−Cu−$DDC^{S1}$ | | | 139 (4) | |
| $His66^{N\epsilon 2}$−Cu−$DDC^{S2}$ | | | 90 (3) | |
| $His66^{N\epsilon 2}$−Cu−$KOJ^{O3}$ | | | | 108 (6) |
| $His66^{N\epsilon 2}$−Cu−$KOJ^{O4}$ | | | | 85 (5) |
| $His68^{N\epsilon 2}$−Cu−$Glu73^{O\epsilon 1}$ | | 86 (5) | | 79 (1) |
| $His68^{N\epsilon 2}$−Cu−$His112^{N\epsilon 2}$ | 114 (4) | 114 (4) | 105 (1) | 106 (5) |
| $His68^{N\epsilon 2}$−Cu−$W^{tb}$ | | 136 (12) | | |
| $His68^{N\epsilon 2}$−Cu−$W^{t}$ | 111 (4) | | | |
| $His68^{N\epsilon 2}$−Cu−$DDC^{S1}$ | | | 99 (2) | |
| $His68^{N\epsilon 2}$−Cu−$DDC^{S2}$ | | | 155 (2) | |
| $His68^{N\epsilon 2}$−Cu−$KOJ^{O3}$ | | | | 92 (10) |
| $His68^{N\epsilon 2}$−Cu−$KOJ^{O4}$ | | | | 158 (5) |
| $Glu73^{O\epsilon 1}$−Cu−$His112^{N\epsilon 2}$ | | 86 (1) | | 84 (7) |
| $Glu73^{O\epsilon 1}$−Cu−$W^{tb}$ | | 80 (5) | | |
| $Glu73^{O\epsilon 1}$−Cu−$KOJ^{O3}$ | | | | 72 (5) |
| $Glu73^{O\epsilon 1}$−Cu−$KOJ^{O4}$ | | | | 97 (2) |
| $His112^{N\epsilon 2}$−Cu−$W^{tb}$ | | 108 (10) | | |
| $His112^{N\epsilon 2}$−Cu−$W^{t}$ | 123 (1) | | | |
| $His112^{N\epsilon 2}$−Cu−$DDC^{S1}$ | | | 123 (2) | |
| $His112^{N\epsilon 2}$−Cu−$DDC^{S2}$ | | | 100 (2) | |
| $His112^{N\epsilon 2}$−Cu−$KOJ^{O3}$ | | | | 146 (7) |
| $His112^{N\epsilon 2}$−Cu−$KOJ^{O4}$ | | | | 94 (5) |

[a] Distances and angles reported here are the average of the values found for the four molecules contained in the asymmetric unit. In parentheses, the standard deviation is given.

$\chi_3 = 48°$ (39°). This conformation is stabilized by a hydrogen bond through the $Glu73^{O\epsilon 1}$ atom with a conserved water molecule at an average distance of 2.6 Å in the four molecules of the asymmetric unit. Among dioxygenases, displacement of a metal ligand has already been observed. In the case of the $Fe^{3+}$-dependent protocatechuate 3,4-dioxygenase, a tyrosinate ligand migrates in response to substrate binding (*32*).

*Crystal Structure of 2,3QD·KOJ.* KOJ, a compound without sulfur atoms, whose chemical structure mimics that of the flavonolic C-ring (Figure 1a,b), was employed to further investigate inhibitor binding to 2,3QD. Figure 2c shows a $2F_o - F_c$ map of the bound inhibitor in the active site. Similarly to DDC, KOJ binds to the metallocenter displacing the solvent ligand. It asymmetrically chelates the Cu ion through its hydroxyl ($KOJ^{O3}$) and carbonyl ($KOJ^{O4}$) oxygen atoms. $KOJ^{O3}$ is at 1.9 Å from the copper while the Cu−$KOJ^{O4}$ distance is 2.6 Å. KOJ adopts approximately the same orientation at the metallocenter as DDC. The major difference is that in 2,3QD·KOJ the $His66^{N\epsilon 2}$−Cu−$KOJ^{O3}$ angle is reduced to 108° as compared to the $His66^{N\epsilon 2}$−Cu−$DDC^{S1}$ angle in 2,3QD·DDC (139°). This orients KOJ toward the Thr53 side chain, to which it is hydrogen bonded through its free hydroxyl group. The position of KOJ is additionally stabilized by a second hydrogen bond between this hydroxyl group and a solvent molecule at 3.0 Å and by van der Waals interactions (Figure 3b).

In the presence of bound KOJ, Glu73 fully coordinates the Cu ion in a syn-monodentate fashion at an average distance of 2.26 Å. Syn-monodentate geometry has been shown to be the most likely arrangement for carboxylate groups when the metal−O distance is below 2.35 Å (*33*). This geometry is partly similar to that observed for the minor position of Glu73 in 2,3QD; the $\chi_1$ and $\chi_2$ angles are almost unchanged (−159° and −140°, and 157 and 150, in 2,3QD and 2,3QD·KOJ, respectively), but the $\chi_3$ angle changes from −168° in 2,3QD to 50° in 2,3QD·KOJ. This rotation moves the $Glu73^{O\epsilon 2}$ atom away from the molecular plane of KOJ. Overall, the copper coordination environment is pseudo-octahedral. From geometrical considerations, the best equatorial plane is the one formed by the ligands provided by His112, His68, and KOJ. Glu73 and His66 are the axial

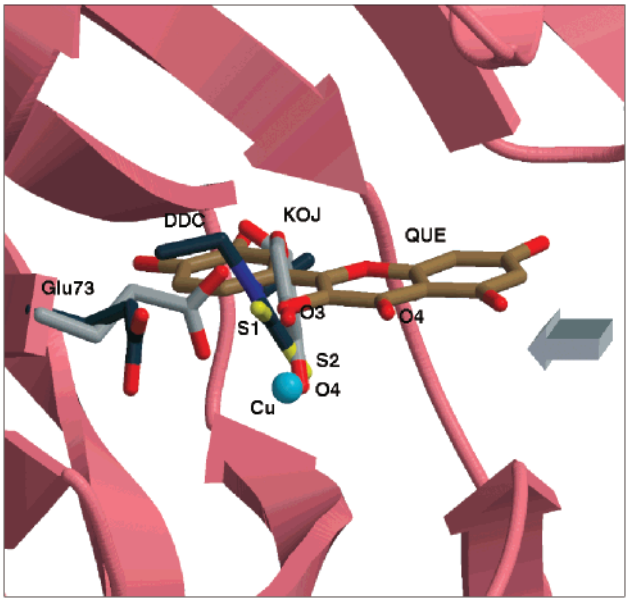


FIGURE 4: Left-side view ("histidine view") of the active site in the presence of the inhibitors DDC (dark gray) and KOJ (light gray) together with the model of the proposed QUE substrate (licorice). The conformations of Glu73 in the presence of the inhibitors are also shown and colored accordingly. The active site entrance is indicated by an arrow.

ligands. The $His66^{N\epsilon 2}$−Cu−$Glu73^{O\epsilon 1}$ angle of 171° is fairly close to the ideal 180°.

Although in the final $\sigma_A$-weighted $2F_o - F_c$ electron density map KOJ molecules are generally well-defined, they display an average *B* factor which is more than twice as high (30.2 Å$^2$) as that of the protein ligands (11.9 Å$^2$) and the copper ion itself (13.0 Å$^2$). Partial KOJ occupancies seem not to be the reason for this, as refinement of KOJ occupancies led to values in the range of 0.85−1.0. Moreover, no appreciable residual positive difference density is observed for Glu73 in nativelike conformations. Therefore, we conclude that the high atomic displacement parameters of the KOJ molecules reflect an intrinsic positional variability. A measure of it is reflected by the standard deviation of the Cu−ligand distances obtained from the four molecules present in asymmetric unit (see Table 2). While all histidine ligands have standard deviations for the Cu−$His^{N\epsilon 2}$ distance below 0.10 Å, the standard deviations for the Cu−$Glu^{O\epsilon 1}$ and Cu−$KOJ^{O3}$ distances are 0.18 and 0.15 Å, respectively. The most variable distance is the Cu−$KOJ^{O4}$ bond with a standard deviation of 0.30 Å. This value is twice as high as the positional rms deviation. Considering that also the $His68^{N\epsilon 2}$−Cu−$KOJ^{O3}$ angle has a high standard deviation (92°(10°), twice the average), it appears that KOJ can adopt a number of similar binding modes. This provides an explanation for its high *B* factor and is also in agreement with the rather poor inhibitory ability of KOJ ($K_i$ in the millimolar range, our unpublished results).

## DISCUSSION

*Inhibition.* Despite their different chemical nature, DDC and KOJ bind the copper ion in a similar way. They asymmetrically chelate the metal with their molecular plane facing the solvent (Figure 4). Compared to KOJ, DDC is tilted by ~25° toward Glu73. Overall, their geometry is perpendicular to that proposed for a quercetin molecule (QUE) bound to the Cu ion (*16*) (Figure 4). Owing to the flavonol-tailored shape of the active site cavity, the B-ring of the flavonol molecule can only be bound deeply buried in the active site (Figure 4) in a pocket lined by the side chains of residues Met51, Thr53, Phe75, Phe114, and Met123. This forces the substrate in a fixed orientation in which the flavonol molecule binds the copper ion only through the $QUE^{O3}$ atom. Because DDC and KOJ do not have such an accessory ring, a perpendicular chelating arrangement, which blocks the inner portion of the cavity, is possible. The geometry displayed by DDC and KOJ appears to be generally achievable by a wide number of small molecules with chelating ability. Among those that have already been proven to inhibit 2,3QD activity (*9*, *30*), toluene-3,4-dithiol and ethylxanthate possess chemical structures compatible with the observed binding mode and are therefore proposed to assume a similar position when coordinated to the metal.

*Ordering of the Cu Center and Glu73 Conformation in the E·S Complex.* The crystal structures determined in this work show that DDC and KOJ induce order in the heterogeneous native copper coordination. This result is consistent with that observed by spectroscopic experiments. EPR measurements (*34*) indicate that upon binding of inhibitors or flavonol substrates the double spectral line of the native enzyme ($g_{II1}$ = 2.330, $A_{II1}$ = 13.7 mT, and $g_{II2}$ = 2.290, $A_{II2}$ = 12.5 mT) changes into a single line ($g_{II}$ and $A_{II}$ values of 2.336 and 11.4 mT, respectively, in the case of the complex with DDC). This suggests a transition from a mixed to a single environment. The present crystallographic work shows that the binding of these inhibitors displaces the positionally variable water ligand and removes the alternate character of the Glu73 side chain. DDC and KOJ induce, however, different non-native Glu73 conformations (Figures 2b,c and 4). In 2,3QD·DDC, the large DDC sulfur atom at a shorter distance from the Cu ion precludes ligation of the Glu73 side chain to the metal. In contrast, in 2,3QD·KOJ, the O-donating KOJ leaves sufficient space for Glu73 ligation. The latter coordination arrangement is particularly interesting. 2,3QD is the first natural copper-containing enzyme for which carboxylate coordination has been observed. However, whereas in the as-isolated enzyme Glu73 coordination amounts to only about 30% occupancy, in 2,3QD·KOJ Glu73 fully coordinates the copper ion. This substantiates the previous observation of copper coordination by a carboxylate side chain and suggests that Glu73 may also coordinate the copper in the E·S complex.

Whereas the shape of the active site clearly suggests the position of the substrate in the complex, docking of quercetin into the active site of 2,3QD could not establish the conformation of the Glu73 side chain, except that its native coordinating conformation is incompatible with the flavonol arrangement, whereas its noncoordinating conformation is less unfavorable (Figure 5). Interestingly, the structure of 2,3QD·KOJ reveals that Glu73 and KOJ can simultaneously ligate the copper ion. Superposition of the modeled 2,3QD·QUE complex and the structure of 2,3QD·KOJ shows that, although the orientation of KOJ is different from that of QUE, the $KOJ^{O3}$ position in the coordination sphere is virtually equivalent to that of $QUE^{O3}$ (Figure 4). This means that, given the chemical identity of the coordinating atoms,

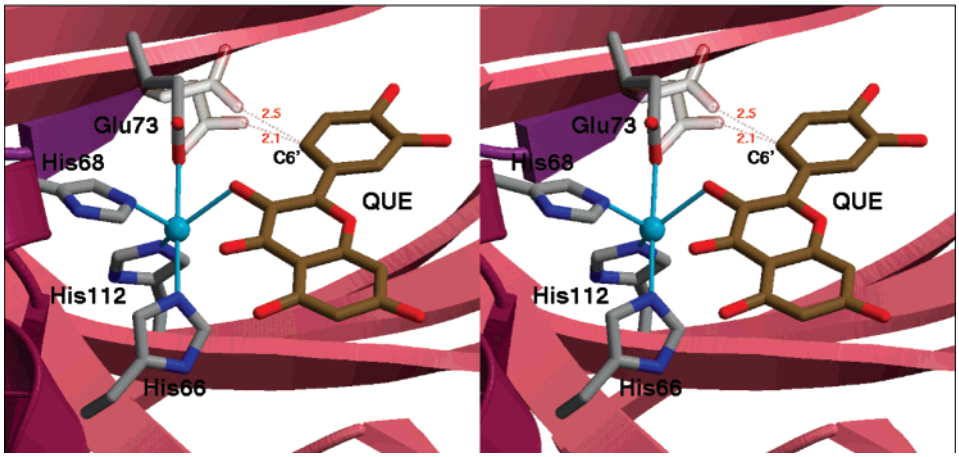


FIGURE 5: Proposed coordination in the E·S complex. The Glu73 conformation observed in the 2,3QD·KOJ complex (gray) is entirely compatible with the modeled QUE positioning (*16*). As a result of the carboxylate rotation, short destabilizing nonbonded interactions between the two observed native positions of $Glu73^{O\varepsilon 2}$ (transparent) and the C6′ atom of the substrate are removed. The resulting geometry is square pyramidal with His68 as apical ligand.

the space occupied at the metal center is very similar for both complexes. Because the KOJ allows for Glu73 coordination, the same necessarily applies to QUE. Moreover, as a consequence of the change in the $\chi_3$ angle, the Glu73 conformation in the complex does not produce any unfavorable nonbonding interactions with the B-ring of the flavonol moiety (in particular with the $QUE^{C6'}$ atom, Figure 5).

A noncrystallographic argument supports our hypothesis that Glu73 is bound to the Cu ion in the E·S complex. XAS measurements have shown that the EXAFS region of the anaerobic 2,3QD·QUE complex is best modeled by three histidine residues and two oxygen atoms (see companion paper). Because substrate modeling in the active site indicates monodentate ligation of the flavonol and only Glu73 is available in the copper environment as an additional O donor, this points to a monodentate coordination of Glu73 in the E·S complex. In this respect, 2,3QD appears fundamentally different from the intradiol-type protocatechuate 3,4-dioxygenase, which requires dissociation of a tyrosine ligand in order for the substrate to bind (*32*).

*Role of Glu73 in the Reaction Mechanism.* Glu73 has been reported to be catalytically important (*16*). Its replacement by a glutamine residue resulted in a 1000-fold reduction of activity. However, it is not yet clear what its specific role is in the reaction mechanism. One proposal has been that Glu73 is the general base that abstracts the flavonol 3−OH proton prior to coordination (*16*). Although deprotonation of the substrate's 3−OH group might, in principle, not necessarily require the presence of an external base as it could be achieved as a consequence of the lowering of the flavonol $pK_a$ induced by metal coordination and solvent exchange, the correct geometric position of Glu73 strongly supports a role for this amino acid in the process.

In light of our observation of the copper ligation by the Glu73 side chain in the presence of the O donor KOJ, we propose as an additional role for this residue that it modulates in the E·S state the redox potential of the $Cu^{2+}/Cu^{+}$ pair. As demonstrated by XAS measurements (see companion paper) and by a nonsilent EPR spectrum (*34*) the copper ion in the 2,3QD·QUE complex is not formally reduced to $Cu^{+}$. However, a $Cu^{+}$−flavonol radical species (Figure 6), whose steady-state concentration is most likely very low, is expected


FIGURE 6: Tautomerism between substrate forms. The activated form is on the right-hand side.

to be the E·S form activated for $O_2$ attack. Different from the $Cu^{2+}$−flavonol species, the $Cu^{+}$−flavonol radical complex possesses two possible sites for dioxygen attack, the flavonol C2 carbon-centered radical and the $Cu^{+}$ center. It is possible that the intrinsic flexibility of the bound Glu73 side chain efficiently tunes during catalysis the valence tautomerism required for the formation of the active $Cu^{+}$−flavonol radical species.

As to Glu73 ligation in the E·S state, it is possible that it occurs either preserving the 3−OH proton abstracted from the flavonol substrate or after assisting its transfer outside the first coordination sphere. In the latter case, a noncoordinating conformation of Glu73 could mimic its conformation in the proton release step. Together, the structures of native 2,3QD and 2,3QD·DDC show that if such an assistance exists, both the interior and the exterior of the active site cavity are accessible for the flexible glutamate side chain; both may provide possible proton acceptors at hydrogen-bonding distance.

## ACKNOWLEDGMENT

The staff scientists operating at beam lines BM14 (EMBL/Grenoble) and BW7B (EMBL/Hamburg) are acknowledged for their help during the experiments.

## REFERENCES

1. Hayaishi, O. (1974) in *Molecular Mechanisms of Oxygen Activation* (Hayaishi, O., Ed.), Academic Press, New York.
2. Broderick, J. B. (1999) *Essays Biochem. 34*, 173−189.
3. Coulter, E. D., and Ballou, D. P. (1999) *Essays Biochem. 34*, 31−49.
4. Bairoch, A. (1993) *Nucleic Acids Res. 21*, 3155−3156.
5. Que, L., Jr. (1999) in *Bioinorganic Catalysis* (Reedijk, J., and Bouwman, E., Eds.) pp 269−321, Marcel Dekker, Inc., New York.
6. Madhusudanan Nair, P., and Vaidyanathan, C. S. (1964) *Biochim. Biophys. Acta 81*, 496−506.

7. Oka, T., and Simpson, F. J. (1971) *Biochem. Biophys. Res. Commun. 43*, 1−5.
8. Sharma, H. K., and Vaidyanathan, C. S. (1975) *Eur. J. Biochem. 56*, 163−171.
9. Hund, H. K., Breuer, J., Lingens, F., Huttermann, J., Kappl, R., and Fetzner, S. (1999) *Eur. J. Biochem. 263*, 871−878.
10. Boldt, Y. R., Sadowski, M. J., Ellis, L. B. M., Que, L., Jr., and Wackett, L. P. (1995) *J. Bacteriol. 177*, 1225−1232.
11. Gibello, A., Ferrer, E., Martin, M., and Garrido-Pertierra, A. (1994) *Biochem. J. 301*, 145−150.
12. Wollenweber, E. (1982) in *Flavonoids: Advances in Research* (Harborne, J. B., and Mabry, T. J., Eds.) pp 189−258, Chapman & Hall, New York.
13. Bors, W., Heller, W., Michel, C., and Saran, M. (1990) *Adv. Exp. Med. Biol. 264*, 165−170.
14. Jovanovic, S. V., Steenken, S., Tosic, M., Marjanovic, B., and Simic, M. G. (1994) *J. Am. Chem. Soc. 116*, 4846−4851.
15. Brown, J. E., Khodr, H., Hider, R. C., and Rice-Evans, C. A. (1998) *Biochem. J. 330*, 1173−1178.
16. Fusetti, F., Schröter, K. H., Steiner, R. A., van Noort, P. I., Pijning, T., Rozeboom, H. J., Kalk, K. H., Egmond, M. R., and Dijkstra, B. W. (2002) *Structure 10*, 259−268.
17. Dunwell, J. M., Khuri, S., and Gane, P. J. (2000) *Microbiol. Mol. Biol. Rev. 64*, 153−179.
18. Abolmaali, B., Taylor, H. V., and Weser, U. (1998) *Struct. Bonding 91*, 91−190.
19. Holm, R. H., Kennepohl, P., and Solomon, E. I. (1996) *Chem. Rev. 96*, 2239−2314.
20. Karlin, S., Zhu, Z. Y., and Karlin, K. D. (1997) *Proc. Natl. Acad. Sci. U.S.A. 94*, 14225−14230.
21. Oka, T., Simpson, F. J., Child, J. J., and Mills, C. (1971) *Can. J. Microbiol. 17*, 111−118.
22. Otwinowski, Z., and Minor, W. (1997) *Methods Enzymol. 276*, 307−326.
23. Schomaker, V., and Trueblood, K. N. (1968) *Acta Crystallogr. B24*, 63−76.
24. Winn, M. D., Isupov, M. N., and Murshudov, G. N. (2001) *Acta Crystallogr. D57*, 122−133.
25. Murshudov, G. N., Vagin, A. A., and Dodson, E. J. (1997) *Acta Crystallogr. D53*, 240−255.
26. Murshudov, G. N., Vagin, A. A., Lebedev, A., Wilson, K. S., and Dodson, E. J. (1999) *Acta Crystallogr. D55*, 247−255.
27. Allen, F. H., Bellard, S., Brice, M. D., Cartwright, B. A., Doubleday, A., Higgs, H., Hummelink, T., Hummelink-Peters, B. G., Kennard, O., Motherwell, W. D. S., Rodgers, J. R., and Watson, D. G. (1979) *Acta Crystallogr. B35*, 2331−2339.
28. McRee, D. E. (1999) *J. Struct. Biol. 125*, 156−165.
29. Laskowski, R. A., Moss, D. S., and Thornton, J. M. (1993) *J. Mol. Biol. 231*, 1049−1067.
30. Oka, T., Simpson, F. J., and Krishnamurty, H. G. (1972) *Can. J. Microbiol. 18*, 493−508.
31. Addison, A. W., Hendriks, H. M. J., Reedijk, J., and Thompson, L. K. (1981) *Inorg. Chem. 20*, 103−110.
32. Orville, A. M., Lipscomb, J. D., and Ohlendorf, D. H. (1997) *Biochemistry 36*, 10052−10066.
33. Glusker, J. P. (1991) *Adv. Protein Chem. 42*, 1−76.
34. Kooter, I. M., Steiner, R. A., Dijkstra, B. W., van Noort, P. I., Egmond, M. R., and Huber, M. (2002) *Eur. J. Biochem.*, in press.
35. Drenth, J. (1999) *Principles of Protein X-ray Crystallography*, 2nd ed., Springer-Verlag, Berlin, Germany.
36. Brünger, A. T. (1992) *Nature 355*, 472−475.
37. Engh, R. A., and Huber, R. (1991) *Acta Crystallogr A47*, 392−400.
38. Esnouf, R. M. (1997) *J. Mol. Graphics 15*, 133−138.
39. Merritt, E. A., and Bacon, D. J. (1997) *Methods Enzymol. 277*, 505−524.
40. Wallace, A. C., Laskowski, R. A., and Thornton, J. M. (1995) *Protein Eng. 8*, 127−134.


BI0159736